Investigation into Transient SFO, FFO, VFTO Overvoltage Characteristics for Typical Gas Insulated Substations

L. Czumbil, J. Kim, H. Nouri

***Abstract*--Overvoltage characteristics of typical single bus, double bus and one and a half bus GIS configurations under transient SFO, FFO and VFTO conditions are studied. The transient conditions are simulated through load rejections, lightning and the opening and closing of circuit breakers or disconnectors. Surge impedance and travel time are used for defining the distributed parameter models of the GIS. The results suggest that for VFTOs the magnitude of the generated overvoltage solely depends on the switching sequences while for SFOs and FFOs the overvoltage depends on the degree of the inductive load and the type and length of transmission lines.**

***Keywords*: Gas insulated substation (GIS), transient overvoltages, SFO, FFO, VFTO, modeling.**

I. Introduction

THE rapid advancement in industrial technologies and population growth during the last decades has considerably increased the energy demand. Due to environmental constraints and reliability of the system Gas Insulated Substations (GIS) have become a major component in today's power networks [1].

The GIS, which is filled with pressurized SF_6 gas for electrical insulation and rapid arc extinction presents a series of advantages against classical air insulated substations, like: small ground space requirements, reduced maintenance, high reliability and protection from pollution. Therefore, these are particularly used in large cities, industrial townships, deserts and arctic areas [2].

Despite these merits, the GIS has its own unique problems. These problems include an increase of overvoltages caused by transient waves reflected from different connections, low surge impedance, and the decreased length of the conductors in these substations. Considering these issues, the propagation of these waves along the conductor will increase compared with conventional substations [3]÷[5].

The paper aims to identify transient overvoltage characteristics of typical Gas Insulated Substations under various transient conditions, namely slow front overvoltages (SFO), fast front overvoltages (FFO) and respectively very fast transient overvoltages (VFTO).

II. GIS Modeling

In order to investigate SFO, FFO and VFTO overvoltage characteristics of typical GIS configurations a 380 kV single power and single outlet GIS is considered (see Fig. 1). On the power side the GIS substation is connected to the grid through a 100 km long single circuit 380 kV/50 Hz overhead line (OHL) to the grid, while on the outlet side the GIS is connected to a medium voltage distribution station with a total load of 100 MVA through a 120 MVA, 380/33 kV star-star configuration transformer and respectively a 10 km long 33 kV transmission line.

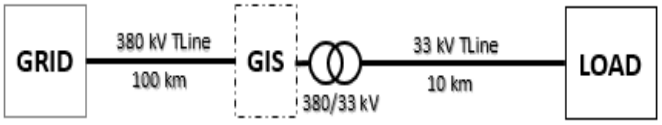

Fig. 1. Investigated GIS substation.

Due to the traveling nature of transients, the investigated GIS is modeled by an equivalent electrical circuit composed by distributed parameter elements. Surge impedance and travel time have been used for defining the distributed parameter model. The inner system, which consists of the high-voltage bus duct and the inner surface of the encapsulation, has been thoroughly represented by line sections, modeled as the distributed parameter transmission lines [1]:

$$Z_S = \sqrt{\frac{L}{C}},\ \tau = \frac{l}{\upsilon},\ \upsilon = \frac{1}{\sqrt{L \cdot C}}, \tag{1}$$

$$L = \frac{\mu_0 \cdot \ln(b/a)}{2 \cdot \pi},\ C = \frac{2 \cdot \pi \cdot \varepsilon_0 \cdot \varepsilon_R}{\ln(b/a)} \tag{2}$$

where: Z_S is equipment surge impedance, τ is travel time, υ is waveform propagation speed, a is bus duct conductor outer radius, b is enclosure inner radius, l is equipment length, L and C are the inductance and capacitance of the equipment, respectively.

Table I presents the obtained surge impedances values for the main GIS components based on equipment geometry:

This work was supported by Hyundai Heavy Industries Co., Ltd. Dong-gu Ulsan, South Korea.

L. Czumbil and H. Nouri are with the Power Systems, Electronics and Control research Laboratory at University of the West of England (UWE), Bristol, U.K.

J. Kim is with Electro Electric Systems Research Institute, Hyundai Heavy Industries Co., Ltd. Dong-gu Ulsan, South Korea and is presently a visiting research scholar at the Power Systems, Electronics and Control research Laboratory, University of the West of England (UWE), Bristol, U.K.

Paper submitted to the International Conference on Power Systems Transients (IPST2015) in Cavtat, Croatia June 15-18, 2015

TABLE I
EQUIVALENT ELECTRICAL PARAMETERS OF GIS COMPONENTS [4]

Component	Notes
GIS Bus Duct	$Z_S = 95\ \Omega$
Disconnectors (DS)	in closed position $Z_S = 42\ \Omega$
	in open position C = 4 pF
Circuit Breakers (CB)	in closed position $Z_S = 66\ \Omega$
	in open position C = 4 pF
Potential Transformers (PT)	$Z_S = 25\ \Omega$, C = 10 pF
Current Transformers (CT)	$Z_S = 42\ \Omega$
Spacers, Elbows	C = 10 pF

For the transient overvoltage studies carried out on the investigated 380 kV gas insulated substation three different GIS configurations were analyzed: a single bus (Fig. 2a), double bus (Fig. 2b) and a one and a half bus (Fig. 2c) configuration, respectively.

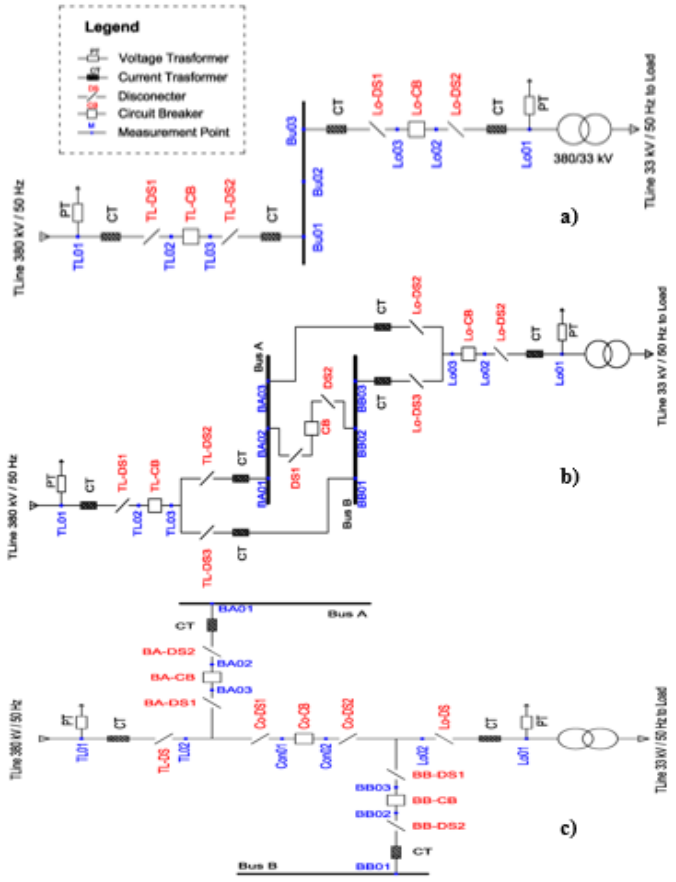

Fig. 2. Investigated GIS configurations: a) single bus GIS; b) double bus GIS; c) one and half bus GIS;

III. SLOW FRONT OVERVOLTAGE STUDY

In high voltage power systems slow front transient overvoltage could be produced by load rejection or phase to ground faults [6], [7].

In the following, the overvoltage seen at the outlet side of the GIS, due to load rejection at the medium voltage distribution station connected to the investigated 380 kV GIS is analyzed. The rejection of different inductive and capacitive loads is studied. Therefore, an 80 MVA load with various inductive and capacitive power factors between 0.97 and 0.4 is rejected while a mostly resistive 20 MVA load (with a power factor of 0.95) is maintained continuously connected to the medium voltage distribution station. The overvoltages at both medium and high voltage sides of the 380/33 kV, 120 MVA transformer placed at the outlet side of the GIS are recorded. Two different scenarios are considered when the medium voltage distribution station is connected to the GIS through an overhead 33kV power line and three single core 33kV underground power cables, respectively. Obtained results are presented in Fig. 3 :

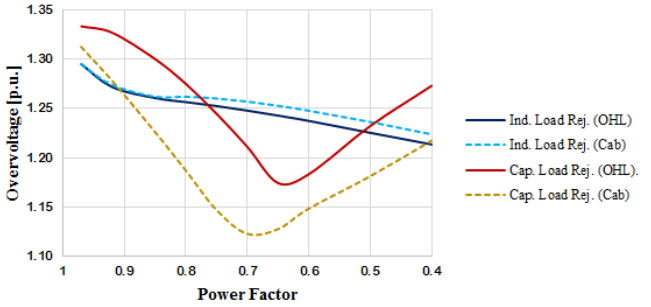

Fig. 3. SFO variation with the power factor of the rejected load.

Fig. 3 presents the variation of the recorded overvoltage at the medium voltage side of the transformer according to the power factor of the rejected inductive and capacitive loads. It can be observed that the rejection of an inductive load produced a 1.25 p.u. overvoltage with a slight decrease with the increase of the inductive part of the rejected load, while the overvoltage produced by the rejection of the capacitive load presents a 'V' curve with a minimum overvoltage at a 0.65 power factor. Higher overvoltage levels could be recorded for the capacitive load rejection when the distribution station is connected to the GIS through the 33kV OHL. Due to the galvanic separation between the two winding of the 380/33 kV transformer the recorded overvoltage at the high voltage side (GIS outlet) is less than 1.05 p.u.

The influence of the transmission line length connecting the medium voltage distribution station to the GIS, on the overvoltage produced by load rejection has also been investigated. The obtained overvoltage values at the medium voltage side for different underground cable and OHL lengths are presented in Fig. 4 and relate to the 100 MVA load of the medium voltage distribution station being rejected:

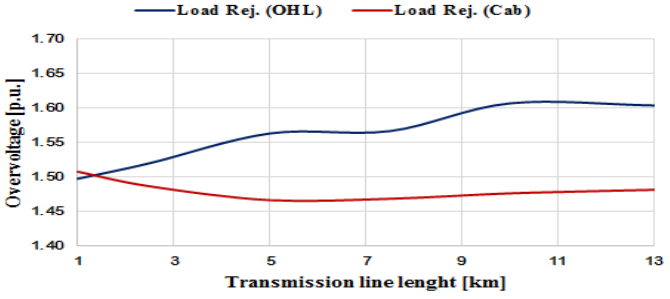

Fig. 4. SFO variation with transmission line length.

IV. Fast Front Overvoltage Study

One of the principal causes of fast front overvoltages in power systems is lightning strike to transmission lines. Lightning overvoltages have a wave head of several micro seconds and are one of the important factors to determine the insulation design of substation equipment, especially in case of GIS. Therefore, in the following the overvoltage seen by the GIS substation at its entrance due to lightning strikes to the 380 kV OHL is investigated. To evaluate lightning overvoltages both direct lightning and back flashover situations are analyzed (see Fig. 5).

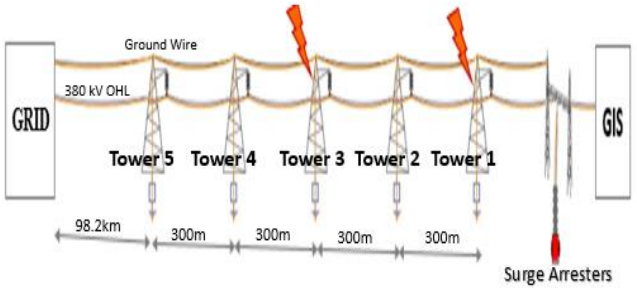

Fig. 5. First five towers of the 380kV OHL modeled for FFO analysis.

For the fast front overvoltage study the first five transmission line towers from the GIS entrance were modeled in detail. The two scenarios when lightning strike hits the first and respectively the third tower from GIS are taken into consideration (see Fig. 5). A combined Hara [8] / Ametani [9] multi-story model has been implemented for the 380 kV delta shape towers to take into consideration both the bracings and the damping effect of each tower section (see Fig. 6). Tower footing is represented by a current dependent variable resistance driven by equation (3) proposed by CIGRE [10] and IEEE [4] to take into account soil ionization phenomena [11].

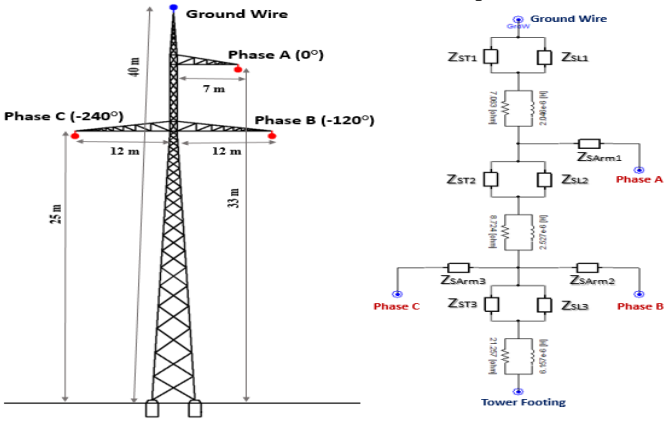

Fig. 6. Delta shape 380 kV tower model

$$R_T = \frac{R_0}{\sqrt{1+\frac{I}{I_C}}};\quad I_C = \frac{1}{2\pi}\cdot\frac{E_0\cdot\rho}{{R_0}^2} \qquad (3)$$

where: R_T is the current dependent tower footing resistance, R_0 is the low current and low frequency footing resistance (10 Ω in our case), I_C is the limiting current to initiate soil ionization, I is the strike current, ρ is the soil resistivity (100 Ω·m) and E_0 is the soil ionization gradient (300 kV/m).

For insulation coordination purposes both situations are investigated when the 380 kV OHL is connected to the GIS substation with and without surge arresters mounted at GIS gantry tower are investigated and obtained overvoltage values are compared to GIS basic insulation level (BIL = 3.5 p.u. considering a 1.1 p.u. safety margin). To model the 420 kV surge arresters the IEEE Std. C62.22 [12] proposed frequency-dependent model (see Fig. 7) has been implemented. Model parameters have been computed based on surge arrester datasheet provided by the manufacturer
(see TABLE II).

TABLE II
SURGE ARRESTER CHARACTERISTICS

System voltage	Rated voltage	Residual voltage	
		10 kA, 8/20 µs	10 kA, 1/5 µs
420 kV	360 kV	783 kV	824 kV

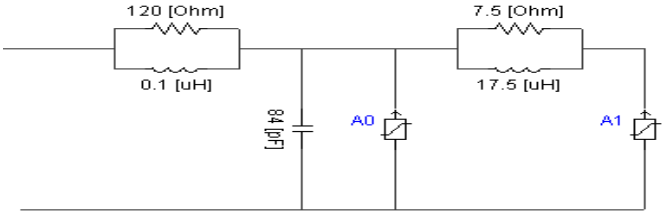

Fig. 7. Implemented IEEE model for 420 kV surge arrester.

A. Direct Lightning

Direct lightning strikes to phase wires in the case of shielded transmission lines could appear in the case of shielding failure. When a relatively low magnitude lightning strike bypasses the overhead ground (shield) wire and attaches to one of the transmission lines phase conductors, shielding failure occurs [13].

Direct lightning due to shielding failure could occur on the upper or the most outward phase wire. The maximum intensity of a lightning strike that could produce shielding failure can be evaluated based on tower geometry, striking distance and the implemented lightning attachment model [14]. For the 380 kV transmission line that connects the investigated GIS substation to the grid, the Eriksson model [15] has been used to evaluate the maximum shielding failure lightning current:

$$I_{MSF} = \left[\frac{\Delta R + \sqrt{\Delta R^2 + \Psi^2\cdot\left(\Gamma^2-1\right)}}{0.67\cdot {H_{PhW}}^{0.6}\cdot\left(\Gamma^2-1\right)}\right]^{1/0.74} \qquad (4)$$

where: I_{MSF} is the maximum shielding failure current in (kA), $\Gamma = \left(H_{GrdW}/H_{PhW}\right)^{0.6}$, $\Psi^2 = \left(H_{GrdW}-H_{PhW}\right)^2 - \Delta R^2$, ΔR is the horizontal distance between phase and grounding wire, H_{GrdW} and H_{PhW} are the height of the grounding and phase wire respectively.

In order to determine the overvoltage at the GIS entrance due to direct lightning strikes to the 380 kV OHL phase conductors, based on the evaluated maximum shielding failure current values (25.6 kA for the upper phase and 20.4 kA for the lower phase wires, respectively), lightning currents with

1/5 µs waveform and an amplitude between 10 kA and 40 kA, are considered using a Heidler function implementation [16]. Two different situations were analyzed: when the lightning strike hits the upper phase wire (phase A see Fig. 6) in the vicinity of the first tower and when it hits nearby the third tower from GIS, respectively (see Fig. 5). For both situations the worst case scenario is applied: lightning hits the wire when the phase voltage reaches its positive peak and thus the maximum overvoltage is produced in the 380 kV OHL. Obtained results are presented in Fig. 8:

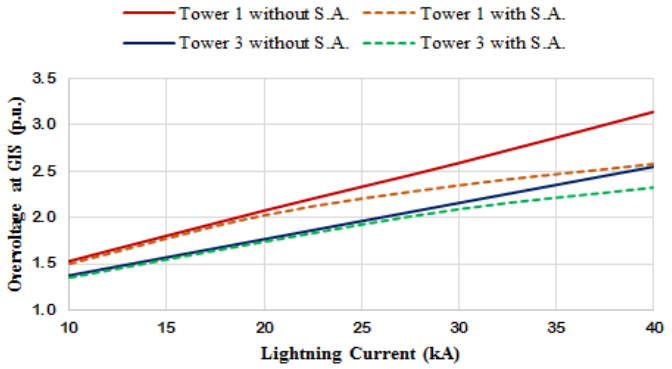

Fig. 8. Maximum overvoltage according to direct lightning current amplitude

Fig. 8 presents the evaluated maximum overvoltage levels at the GIS entrance with and without surge arresters mounted on the 380 kV OHL at GIS entrance. In the worst case scenario a 3.14 p.u. overvoltage is recorded for a 40 kA, 1/5 µs lightning current (which is almost double that the evaluated maximum shielding failure current), and this could be reduced to 2.58 p.u. by placing surge arresters at the GIS entrance. For less than 20 kA, respectively 25 kA direct lightning strikes near the first tower and respectively the third tower or further away the produced overvoltage levels at the GIS entrance will be even lower than the discharge voltage of the surge arrester. Fig. 9 represents the overvoltage waveform observed at the GIS entrance for 40 kA and 20 kA lightning strike currents with and without surge arresters mounted at the GIS entrance:

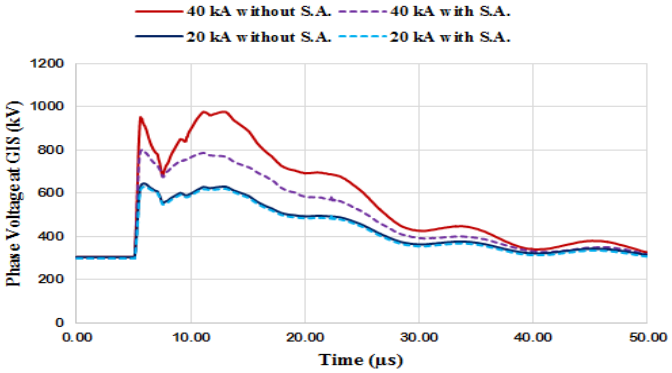

Fig. 9. Phase voltage at GIS entrance in case of direct lightning

B. *Back Flashover*

In order to evaluate the overvoltage seen at the GIS entrance due to back flashover on the 380 kV overhead transmission line connected to the GIS, a 200 kA lightning current with a 8/20 µs waveform is considered. The black flashover mechanism has been modeled by an open switch in parallel to the phase wire insulator string capacitance. Once the voltage across the insulator string reaches the withstanding capability of the insulator, back flashover occurs and the switch is closed.

Due the fact that the insulator string may withstand a high transient voltage for a short duration, but it could fail to withstand a lower transient voltage with a longer duration, the volt-time characteristic proposed by CIGRE [10] has been implemented for the back flashover simulations:

$$V_{WIns} = K_1 + \frac{K_2}{t^{0.75}} \qquad (5)$$

where: V_{WIns} is the insulator string withstand voltage in (kV), $K_1 = 400 \cdot L$, $K_2 = 710 \cdot L$, L is the length of the insulator string in (m), and t is the elapsed time in (µs) from the lighting strike occurring.

Two different situations were investigated: when the lightning strike hits the ground wire at the first tower from the GIS substation (Tower 1 see Fig. 5) and respectively when the lightning hits the ground wire at the third tower (Tower 3). For both situations the phase overvoltage at the GIS entrance has been evaluated with and without surge arrestors mounted at the 380 kV OHL gantry tower. In order to obtain the highest overvoltage values that could occur due to back flashover the worst case scenario is applied: the lightning strike hits the tower when the phase voltage on the upper conductor (phase A) reaches its negative peak. In this situation voltage across the insulator string reaches its withstand capability earlier. Computed overvoltage waveforms are presented in Fig. 10:

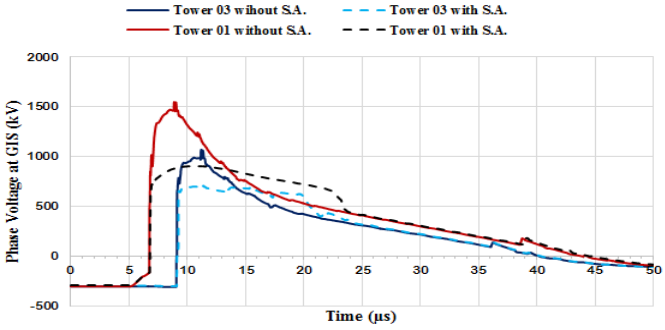

Fig. 10. Phase voltage at GIS entrance in the case of back flashover.

It can be observed that the highest 4.97 p.u. overvoltage (1546 kV) occurs when the lightning strike hits the first tower (no surge arrester). If the lightning hits the third tower the overvoltage impulse needs a 2 µs travel time to reach the GIS entrance and it is reduced to 3.44 p.u. (1069 kV). By mounting surge arresters at the GIS entrance these overvoltage values will be reduced to 2.9 p.u. and 2.3 p.u. respectively, lower than the basic insulation level of the GIS (3 p.u.).

V. Very Fast Transient Overvoltage Study

Very fast transient overvoltage could be generated in GIS substations during the opening and closing of circuit breakers or disconnectors [6]. The disconnector restriking surge is an oscillation surge with a very high frequency of several MHz.

The frequency of the disconnector restriking surge is much higher than that of lightning surges because every disconnector operation potentially generates the overvoltage, and the surge could impose negative effects not only on the main circuit insulation but also on a secondary system such as EMC [17], [18].

Therefore, all the possible disconnector and circuit breaker closing switching operations have been analysed for the three investigated GIS configurations (single bus Fig. 2a, double bus Fig. 2b and one and a half bus Fig. 2c). It is considered that the switching order for a feeder connected to the main bus is closing the disconnectors and then the circuit breaker.

During the closing operation of a disconnector (DS) or circuit breaker (CB), the sparks are modeled by a fixed resistance in series with an exponentially decreasing one:

$$R(t) = R_0 + R_1 \cdot \exp\left(-\frac{t}{\tau}\right) \qquad (6)$$

where: $R_0 = 0.5\Omega$, $R_1 = 10^6\,\Omega$ and $\tau = 1ns$.

Obtained overvoltage values due to DS and CB switching were analyzed at several measurement points along the investigated GIS configurations (see Fig. 2).

A. Single Bus Configuration

Analyzing all the possible disconnector and circuit breaker switching inside the single bus configuration GIS revealed that the highest VFTO value is produced by switching (closing) the 380 kV TLine feeder circuit breaker with the load side feeder connected to the bus duct. Fig. 11 presents the overvoltage waveform recorded in the middle of the main bus during the switching operation:

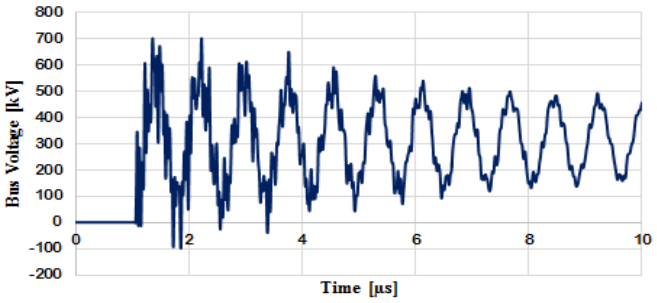

Fig. 11. GIS overvoltage produced by switching 380 kV TLine side CB.

In order to energize the outlet of the investigated GIS from the 380kV transmission line the following sequence of closing switching operations has been identified for the single bus GIS configuration:

OP01. Closing Load side DS1, DS2 and CB - Closing 380 kV TLine side DS1, DS2 and CB;

OP02. Closing 380 kV TLine side DS1, DS2 and CB - Closing Load side DS1, DS2 and CB;

Fig. 12 presents the produced maximum overvoltage levels inside the one bus GIS and the number of energized switching need by each of the above presented closing operation sequences.

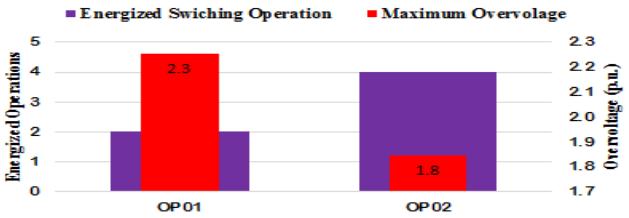

Fig. 12. Maximum overvoltage / number of energized switching for the one bus GIS configuration.

B. Double Bus Configuration

If Bus B of the double bus GIS configuration is totally disconnected from the 380 kV TLine feeder, Load feeder and respect Bus A (see Fig. 2b) than the double bus GIS will work in a one bus configuration similar to that presented above. In this case the overvoltage introduced by switching the 380 kV TLine feeder CB is reduced to 2.31 p.u. Fig. 13 presents the overvoltage waveform recorded at Bus A, measurement point 2 (in the middle of Bus Duct A see Fig. 2b):

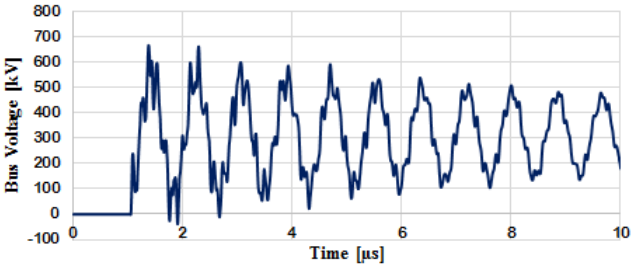

Fig. 13. GIS overvoltage produced by switching 380 kV TLine side CB.

In order to energize the outlet of the investigated GIS from the 380kV transmission line the following sequence of closing switching operations has been identified for the double bus GIS configuration (see Fig. 2b):

OP01. Closing Load side DS1, DS2 and CB - Closing 380 kV TLine side DS1, DS2 and CB (energizing the load side through Bus A with Bus B disconnected);

OP02. Closing 380 kV TLine side DS1, DS2 and CB - Closing Load side DS1, DS2 and CB (energizing the load side through Bus A with Bus B disconnected);

OP03. Closing Load side DS1, DS3 and CB - Closing 380 kV TLine side DS1, DS3 and CB (energizing the load side through Bus B with Bus A disconnected);

OP04. Closing 380 kV TLine side DS1, DS3 and CB - Closing Load side DS1, DS3 and CB (energizing the load side through Bus B with Bus A disconnected);

OP05. Closing Load side DS1, DS2 and CB - Closing 380 kV TLine side DS1, DS2 and CB (energizing the load side through Bus A with Bus B already connected to Bus A);

OP06. Closing 380 kV TLine side DS1, DS2 and CB - Closing Load side DS1, DS2 and CB (energizing the load side through Bus A with Bus B already connected to Bus A);

OP07. Closing 380 kV TLine side DS1, DS3 and CB - Closing Load side DS1, DS3 and CB (energizing the load side through Bus A with Bus B already connected to Bus B);

OP08. Closing Load side DS1, DS3 and CB - Closing 380 kV TLine side DS1, DS3 and CB (energizing the load side through Bus B with Bus A already connected to Bus B);

Fig. 14 presents the produced maximum overvoltage levels inside the double bus GIS and the number of energized switching need by each of the above presented closing operation sequences.

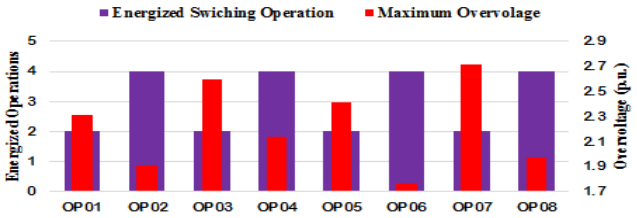

Fig. 14. Maximum overvoltage / number of energized switching for the double bus GIS configuration.

From Fig. 14 it can be observed that closing sequence OP06 produces the lowest overvoltage level in the double bus GIS configuration (1.76 p.u.) but it needs 4 energized switchings, while sequence OP1 needs only two energized switching with a maximum overvoltage of 2.31 p.u.

C. One and a Half Bus Configuration

In the case of the one and a half bus GIS configuration (Fig. 2c) the following sequence of closing switching operations has been identified:

OP01. Closing Load side DS - Closing 380 kV TLine to Load DS and CB - Closing 380 kV TLine DS with both bus bars disconnected;

OP02. Closing 380 kV TLine to Load DS and CB - Closing 380 kV TLine DS - Closing Load side DS with both bus bars disconnected;

OP03. Closing Load side DS - Closing 380 kV TLine DS - Closing 380 kV TLine to Load DS and CB with both bus bars disconnected;

OP04. Closing 380 kV TLine DS - Closing 380 kV TLine to Load DS and CB - Closing Load side DS with both bus bars disconnected;

OP05. Closing Load side DS - Closing 380 kV TLine to Load DS and CB - Closing 380 kV TLine DS with both bus bars already connected;

OP06. Closing 380 kV TLine to Load DS and CB - Closing 380 kV TLine DS - Closing Load side DS with bus bars already connected;

OP07. Closing Load side DS - Closing 380 kV TLine DS - Closing 380 kV TLine to Load DS and CB with both bus bars already connected;

OP08. Closing 380 kV TLine DS - Closing 380 kV TLine to Load DS and CB - Closing Load side DS with both bus bars already connected;

Fig. 15 presents the produced maximum overvoltage levels inside the one and half bus GIS and the number of energized switching need by each of the above presented closing operation sequences.

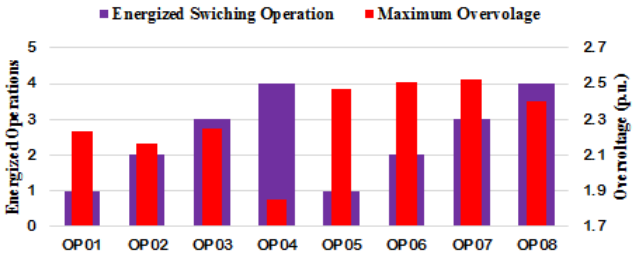

Fig. 15. Maximum overvoltage / number of energized switching for the one and a half bus GIS configuration.

From Fig. 15 it can be observed that closing sequence OP04 produces the lowest overvoltage level in the one and half bus GIS configuration (1.85 p.u.) but it needs 4 energized switching, while sequence OP1 needs only one energized switching with a maximum overvoltage of 2.23 p.u.

VI. Conclusions

Overvoltages produced by the rejection of inductive loads decrease slightly with the increase of the inductive part of the rejected loads, while overvoltages produced by the rejection of the capacitive load exhibits a 'V' curve.

Different line length cables and/or overheads connecting the medium voltage distribution station to the GIS have revealed that the overvoltage produced by the overhead line is greater.

The combined Hara [8] and Ametani [9] multi-story tower model considers both the bracings and the damping effect and used in conjunction with an adaption of CIGRE tower footing variable resistance yields realistic results.

Results from all possible disconnectors and circuit breakers closing switching operations for the three GIS configurations show that the switching sequence plays a significant role in the magnitude of the generated overvoltage. For example, for single bus, double bus, one and a half bus GIS configurations, the switching operations OP02, OP06 and OP04, respectively, generate the minimum overvoltage.

VII. References

[1] A. Tavakoli, A. Gholami, H. Nouri, M. Negnevitsky, "Comparison Between Suppressing Approaches of Very Fast Transients in Gas-Insulated Substations (GIS)", *IEEE Trans. on Power Delivery*, vol. 28, pp. 303-310, January 2013.

[2] G. H. C. Oliveira, S. D. Mitchell, "Comparison of Black-Box Modeling Approaches for Transient Analysis: A GIS Substation Case Study", in *Proc. International Conference on Power System Transients, (IPST)*, Vancouver, Canada, 18-20 July, 2013.

[3] M. M. Rao, M. J. Thomas, B. P. Singh, "Frequency Characteristics of Very Fast Transient Currents in a 245-kV GIS", *IEEE Trans. on Power Delivery*, vol. 20, pp. 2450-2457, October 2005.

[4] IEEE Fast Front Transients Task Force, "Modeling Guidelines for Fast Front Transients", *IEEE Trans. on Power Delivery*, vol. 11, pp. 493-506, January 1996.

[5] J. Mahseredjiana, S. Dennetièreb, L. Dubéc, B. Khodabakhchiand, L. Gérin-Lajoiee, "On a New Approach for the Simulation of Transients in Power Systems", *Electric Power Systems Research*, vol. 77, pp. 1514 – 1520, September 2007.

[6] IEEE Std. 1313.2, "IEEE Guide for the Application of Insulation Coordination", IEEE-SA Standards Board, 1999.

[7] IEC 60071-2, “Insulation Coordination - Part 2: Appication Guide”, *International Electrotechnical Commission, (IEC)*, Geneva, Swizerland, 1996.

[8] T. Hara, O. Yamamoto, “Modelling of a Transmission Tower for Lightning Surge Analysis”, *IEE Proc. - Generation, Transmission and Distribution*, vol. 143, pp. 283-289, May 1996.

[9] A. Ametani, T. Kawamura, “A Method of a Lightning Surge Analysis Recommended in Japan Using EMTP”, *IEEE Trans. on Power Delivery*, vol. 20, pp. 867-895, April 2005.

[10] CIGRE WG33.01, “Guide to Procedures for Estimating the Lightning Performance of Transmission Lines”, CIGRE Technical Report 063, October 1991.

[11] Z. G. Datsios, P. N. Mikropoulos, T. E. Tsovilis, “Impulse Resistance of Concentrated Tower Grounding Systems Simulated by an ATPDraw Object”, in *Proc. International Conference on Power System Transients, (IPST)*, Delft, Netherlands, 2011.

[12] IEEE Std. C62.22, “IEEE Guide for the Application of Metal-Oxide Surge Arresters for Alternating-Current Systems”, *IEEE-SA Standards Board*, New York, USA, 2009.

[13] IEEE Std. 1243, “Guide for Improving the Lightning Performance of Transmission Lines”, June, 1997.

[14] P. N. Mikropoulos, T. E. Tsovilis, “Lightning Attachment Models and Maximum Shielding Failure Current of Overhead Transmission Lines: Implications in Insulation Coordination of Substations”, *IET Generation, Transmission & Distribution*, vol. 4, pp. 1299-1313, December, 2010.

[15] A. J. Eriksson, “An improved electrogeometric model for transmission line shielding analysis”, *IEEE Trans. Power Delivery*, vol. 2, no. 3, pp. 871–886, 1987.

[16] A. Ceclan, V. Topa, D.D. Micu, A. Andreotti, “Lightning-Inverse Reconstruction by Remote Sensing and Numerical-Field Synthesis”, *IEEE Trans. on Magnetics*, vol. 49 , no. 5, pp. 1657-1660, May 2013.

[17] H. C. Seo, W. H. Jang, C. H. Kim, T. Funabashi, T. Senju, “Analysis of rate-of-rise of VFTO according to Switching Conditions in GIS”, in *Proc. International Conference on Power System Transients, (IPST)*, Delft, The Netherlands, 14-17 June, 2011

[18] L. Zhang, Q. Zhang, S. Liu, F. Liu, “Insulation Characteristics of 1100 kV GIS under Very Fast Transient Overvoltage and Lightning Impulse”, *IEEE Transactions on Dielectrics and Electrical Insulation*, vol. 19, no. 3, pp. 1029-1036, June 2012.